Perkins&Will

Research Journal

2015 / VOL 07.02

SPECIAL ISSUE: FUTURE OF ARCHITECTURAL RESEARCH

ARCHITECTURAL RESEARCH CENTERS CONSORTIUM 2015 CONFERENCE

01.
DESIGNED FOR PERFORMANCE:
Research Methods in a Collaborative Studio Rethinking Modern Curtain Walls

Michael Gibson, Kansas State University, Assoc. AIA, LEED AP,
mdgibson@ksu.edu

ABSTRACT
The growing demand for high-performance buildings has pushed the architectural discipline to confront building performance as an integral part of design delivery, while increasing the necessity of collaboration between designers, building science experts, engineers, and manufacturers to find the best solutions to building performance challenges. At Kansas State University, a year-long research studio worked with professionals, consultants, and a major manufacturer of window systems to rethink modern curtain wall systems. Three experimental systems developed during the studio are summarized in this article along with data and observations showing their relative successes and shortcomings versus a contemporary high-performing curtain wall system. This article elaborates on methods employed in the studio including computer-based analysis and in-situ testing of full scale prototypes with emphasis on determining and comparing apparent thermal resistance calculated from observations. Lastly, some discussion is presented regarding how these methods and techniques could contribute to practice.

KEYWORDS: envelopes, performance, simulation, testing, prototyping

1.0 INTRODUCTION

Designing high-performance buildings requires architects to engage building science and manufacturing in a more direct way than in the recent past, where a handful of material properties were enough to inform decisions. Today, architects are poised to work with consultants, engineers, and manufacturers to improve solutions to building performance challenges. Coincidentally, architects are uniquely positioned to innovate in this area because the profession bridges between the technical aspects of building and the performance objectives driving projects. In the area of building skins, the intersection of technology and multivalent performance is particularly acute: skins have to resist heat flow, control moisture, shade the interior, provide views, resist wear and decay, and contribute to the identity of the building. Decisions with respect to the building skin are complex, often revealing gaps in the knowledge of how these building systems behave. Architects can do more than just identify these gaps – it is possible to use a foundation of building science knowledge, rigorous research methods, and a collaborative approach to innovate in these areas.

This article summarizes work from a year-long architectural studio in the Department of Architecture at Kansas State University that engaged a team of practitioners from BNIM and PGAV (Kansas City architecture firms), outside engineers and specialist consultants, and a regional curtain wall manufacturer in a research and design project during the 2014-15 academic year. Students worked in teams in the fall of 2014 to develop experimental curtain wall systems intended to advance the thermal performance of today's best contemporary glass curtain wall systems, questioning material, environmental integration, and manufacturing implications of the systems they developed. In the studio, students were also introduced to a research approach based on building science concepts, experimental methods, simulation and analysis tools, and prototyping. The studio's work culminated with the live testing of their experimental systems, which they constructed at 1:1

scale and deployed in an instrumented test enclosure. In the spring of 2015, the students continued the work of the studio by designing a library branch: a realistic project where they further developed their experimental systems in detail (not discussed in this article). The collaborating architects, consultants, and manufacturer representatives provided feedback during both semesters. A more detailed discussion of the studio's work was previously published[1]. This article examines the testing and analysis methods behind the work in greater detail, while restating and expanding earlier interpretations of how the three systems presented performed.

2.0 CURTAIN WALLS: PERFORMANCE CHALLENGES AND POTENTIAL SOLUTIONS

The performance associations of glass and aluminum curtain walls is certainly mixed today. Critics pan highly glazed buildings purported as "green" by their owners and designers, referring to the expectedly poor thermal performance of glass walls versus opaque construction depended on insulation products to reduce thermal transmission. The performance reality of large glass walls in green buildings is quickly changing, however. The best-performing glass systems achieving rated U-Values approaching 0.125 BTU/hr-ft^2-°F, a level of thermal resistance on par with an insulated 2"x4" stud wall. Another widely misunderstood reality of curtain walls today is determining which components comprise the weak areas in the assembly. Decades ago, when thermally-broken metal framing became popular, the glass units were more challenging thermally. Yet glazing technologies (triple pane, argon-fill, low-E coated) can produce an insulated glass unit with a thermal resistance that can be many times greater than that of the frames. Curtain wall manufactures have thus invested heavily in producing the best insulated glass units possible. Yet the frames in curtain walls have remained unchanged for decades, descending nearly directly from profiles engineered in the mid-20th century and opened to free use when the intellectual property rights ceased in the 1980s. As a result, the frames remain as an important area for improving these systems.

Some of the biggest energy challenges with glass and aluminum curtain wall systems involve thermal performance. Thermal breaks reduce conduction, using new materials, such as polyamide that preserve the structural stability of the frames, but conduct heat much less readily than aluminum. Gasketing and sealing further prevent conduction as well as provide the airtightness to reduce infiltration and exfiltration. Lastly, the system's real-life performance can be compromised by poor detailing and installation methods, which are usually not represented in a particular system's thermal ratings[2]. Other energy challenges involve the production of high-quality glass and the demand for anodized coatings, which require high-quality "virgin" (unrecycled) aluminum.

2.1 Performance Advantages of Modern Curtain Walls

The advantages of these systems, however, are numerous. First, the systems are affordable, with a kit-of-parts erection process and clear expectations for performance (thermal and otherwise) when comparing to layered walls, such as veneer masonry that relies on complex, difficult-to-control, and difficult-to-inspect layers involving insulation, narrow air cavities, hangers, ties, and flashing. Secondly, curtain wall systems can also be very airtight in comparison to traditional fenestration systems where the layered envelope can be a challenge to seal. A recent assessment of the role of infiltration in energy use of commercial buildings developed a target infiltration rate used for energy models of 1.2 L/s-m^2 (0.24 cfm/ft^2) @ 75 Pa (1.58 psi), based on modern construction data with a "best achievable" infiltration rate of 0.2 L/s-m^2 (0.04 cfm/ft^2) @75 Pa (1.58 psi)[3]. Only six percent of a set of existing buildings tested met the target standard for infiltration[3]. The same study estimates that reducing infiltration rates in commercial buildings to the target rate would save 40 percent in natural gas and 25 percent in electrical energy in heating dominated climates. Consequently, the biggest infiltration problem areas in buildings comes from interfaces between fenestration and opaque walls, and one may surmise that buildings can be made tighter by avoiding the wall system of "punched" openings encouraged by prescriptive codes (and window-wall ratios) and use continuous systems where airtightness can be best maintained. The triple glazed curtain wall system available from the collaborating manufacture infiltrates at 0.06 cfm during a standard test at 6.24 psf; if the system could maintain such tightness continuously across an entire building envelope it could easily perform below the established targets[3].[i]

[i] This comparison is based upon different tests (whole building infiltration versus assembly infiltration) and does not address the challenge of establishing continuity at floors, roofs, and other challenging areas, especially when required by tall buildings. Yet the potential for high-performing glazed curtain wall systems to outperform conventional layered walls is very strong when reduction of infiltration is considered.

3.0 STUDIO RESEARCH PROCESS AND METHODS

The studio's research model reflects aspects of several current research trends in academia and practice. The collaborating manufacturer in the project supported the students' research effort by providing materials and knowledge, but without a formal research stake in the project – similar to other open-ended "sponsored studios" taking place elsewhere in the academy. Yet, the studio sought to focus not just on experimentation, but also on advanced research tools and methods that could potentially bridge between the profession of architecture and performance-driven manufacturing. While taking inspiration from programs at other academic research centers, such as the Integrated Design Lab (University of Washington and University of Idaho) and High Performance Building Laboratory (Georgia Institute of Technology), the studio sought to demonstrate research process and outcomes that could be initiated and carried out in practice, instead of engaged in a specialized institution or lab. Considering this aim, the methods and tools of the studio are readily available to professionals at relatively low cost including widely available computer simulation software, but also the instrumentation used to perform in-situ testing. In summary, one might think of the student teams as design teams within any architect's office, given the latitude to study a particular performance problem involving a manufacturer, with architectural integration serving as a final objective. The trajectory of the students towards architectural integration played out in the studio with the students ultimately designing their experimental curtain wall systems into their design projects in the spring semester, where they finalized architectural detailing and worked their systems into their design concepts.

Beginning with a phase of background research and tours of the collaborating manufacture's facility in Manhattan, Kansas, the students formed teams of three students each, for a total of five teams, and proceeded to develop experimental curtain wall systems offering improved thermal performance. The experimental systems were evaluated at each stage of development against the manufacturer's 2.5-inch profile aluminum curtain wall system (referred to in the text as 250xpt), with polyamide thermal breaks and triple-glazed, argon-filled IGUs. Work began in a "what if" stage, where hypotheses were developed by the teams with respect to system performance and the physics of thermal efficiency, considering also material capabilities and structure.

3.1 Computer Simulation

Computer simulation was used in the earliest stages of experimental system development. Initially teams worked with THERM and WINDOW, two simulation programs developed by the Lawrence Berkeley National Laboratory, to analyze two-dimensional model sections. In this software, finite element analysis calculates multiple modes of heat transfer through the section, given prescribed environmental conditions at each side of the wall. Students used NRFC simulation configurations and boundary conditions to compare their systems' performance to the manufacturer's official NFRC certification models, as the National Fenestration Ratings Council (NFRC) uses this software in its certification process. Virtual testing at this stage also permitted student teams to easily test multiple configurations of their systems at one time, optimizing designs as they received feedback from the simulation programs, much like manufacturers do when developing new products. THERM and WINDOW models calculate thermal properties for an enclosure system, such as U-Value, Solar Heat Gain Coefficient, and Visible Transmittance; yet it is also important to understand how these thermal properties affect building performance when they contribute to overall building loads. In order to evaluate this impact, the studio used whole building energy simulations (carried out in Autodesk Ecotect) where a 24,000 square foot skin-load dominated office building was modeled according to IECC prescriptive guidelines. Set in Des Moines, Iowa (IECC Zone V) with 38 percent window-to-wall ratio and realistic internal and ventilation loads, these simulations showed how the experimental systems might improve overall building efficiency.

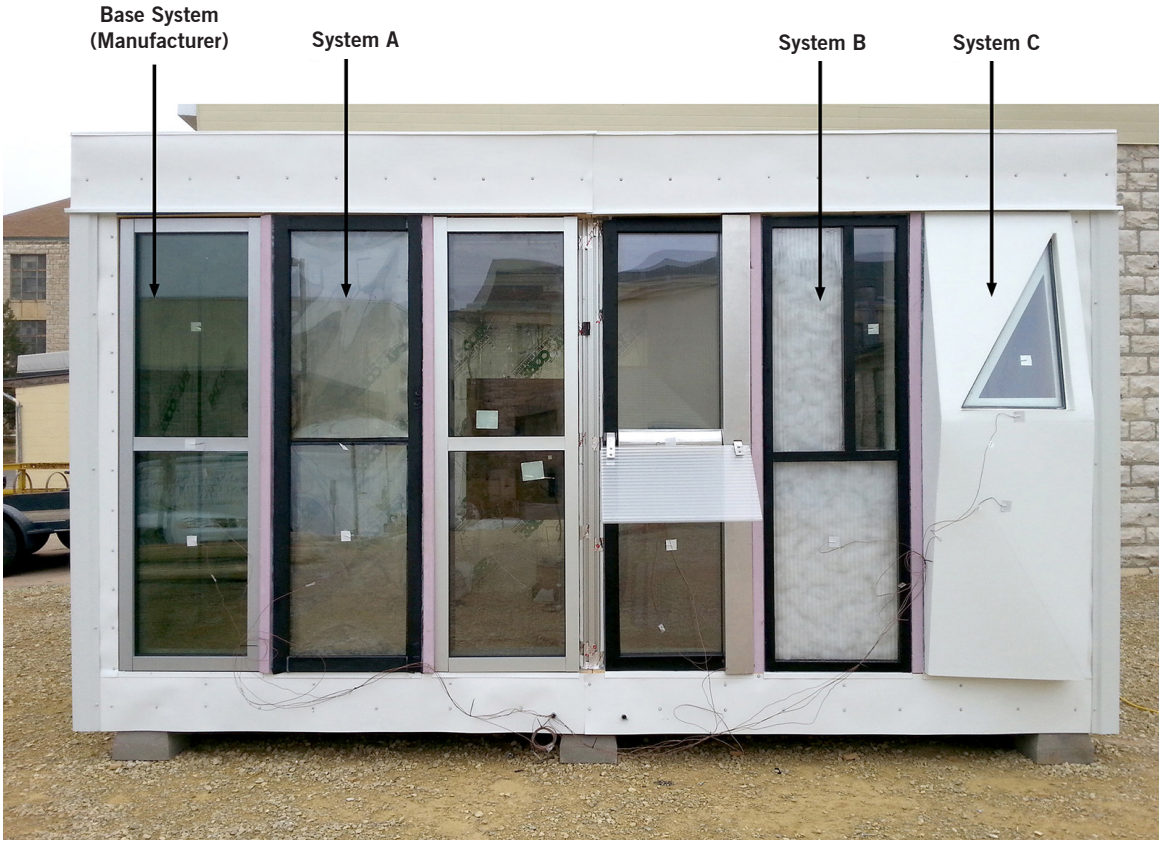

Figure 1: Image showing test structure and 1:1 scale prototypes constructed by the students for thermal testing.

3.2 Prototyping

The last phase of development involved the production of prototypes, built at 1:1 scale after the student teams had vetted their experimental systems via computer analysis. The first prototypes were "desktop models" that served as a proof-of-concept and helped students to understand the material and assembly implications of their proposals. The final prototypes built by the students were constructed to fill a 27 inch wide by 74 inch high opening in a specially constructed test enclosure (Figure 1). The large prototypes were intended first to demonstrate material and assembly concepts, but were also installed in the test enclosure so that real-world thermal performance could be evaluated alongside the manufacturer's 250xpt curtain wall unit. Testing at this scale intended to test the typical, most frequently occurring joints in the curtain wall – though it may be mentioned that thermal transfer in curtain wall weak points such as building corners and expansion zones was not part of the scope of prototyping and testing.

In order to fabricate the large mockups, the teams were forced to make substitutions in their materials and thus some difference would exist between the mock ups and the virtual tests conducted earlier. In the test enclosure, the curtain walls faced south with maximum solar exposure, with the remaining walls of the test enclosure were composed of 3.5 inch structural insulated panels with an additional 0.75 inches of polystyrene insulation over the exterior (see notes for more information on test house construction) with all joints double sealed with foil tape. Lastly, a thermostatically controlled electric heating unit was used during tests to heat the interior of the roughly 1000 cubic foot volume (16' x 8' x 8'), using a low velocity fan and directed away from any of the prototypes and temperature sampling sites. Testing in the enclosure during the winter of 2014-15 involved a

number of experiments where temperatures at specific points on the prototypes were monitored as well as a series of infiltration tests to measure air leakage through the prototypes.

3.3 Testing Apparent Thermal Resistance

The goal of monitoring temperatures in the prototypes was to compare the apparent thermal resistance of six systems at similar locations in the glass units and center mullions. It is important to emphasize the distinction between apparent thermal resistance and resistance (i.e. R-Value) calculated by computer simulation or provided in material ratings, the latter two being somewhat idealized. It was expected that the apparent resistance of the systems would be different from those calculated by THERM and WINDOW, although the relative order or performance (most to least thermal resistance) would persist in the live tests. Additionally, the studio's tests referenced ASTM standards related to measuring temperature (ASTM C1046-95) and determining heat flux from in-situ data (ASTM C1155-95) in some respects, but could not follow the standards set in ASTM C1155-95) for calculating thermal resistance because of the lack of heat flux sensors among the instruments used[4,5]. Further discussion of heat flux sensors is made in the notes; one of the attempts of the research was to use easier-to-acquire temperature data without heat flux meters to calculate apparent thermal resistance. The validity of this method is certainly open for interpretation and more work is needed to establish the accuracy of using only temperature data to evaluate building components in-situ[ii,iii].

[ii] The test enclosure was constructed using aluminum structural components and enclosed using 3.5in SIP panels with polyurethane insulating cores. With an additional 0.75 inches of continuous insulation the envelope was increased to a thermal resistance of R 28.3 ft2-°F-hr/Btu. Interfaces between structure and envelope panels used gaskets that were compressed as panels were bolted together. All gaps were taped and any accessible gaps were filled with loose foam and backer rod. Prototypes were installed over steel sill flashing and were separated by a two inch of extruded polystyrene (0.75 inchs of expanded polystyrene at the edges), and all gaps were sealed with backer rod and silicon caulk.

[iii] Data collected during thermal tests referenced ASTM C1046-95 (2013) and ASTM C1155-95 (2013), but as noted did not use heat flux sensors to measure heat flux. A single heat flux sensor would provide a precise measure of heat flux (q) for any given temperature sampling site, and the resistance of the envelope (R_{envp}) could be solved with only the observed interior and exterior surface temperatures at that site. However, heat flux sensors are many times more expensive than thermocouples, and data acquisition required to log these sensors is also more expensive and challenging, involving signal processing at the microvolt scale. For the experimental setup used in the studio, where fourteen individual sampling sites were monitored on both inside and out, using so many heat flux sensors was not possible. It may be possible in the future to use one heat flux sensor and some process of interpolation to make resistance calculations more accurate for multiple locations, but this methodology requires further evaluation. Research on how to conduct in-situ thermal resistance tests economically (i.e. by students and designers) is ongoing.

Temperatures from the thermocouples were recorded at five second intervals using synchronized data acquisition and a laptop during tests[iv], and the tests were conducted for several hours without disturbance, focusing on nighttime periods with cold temperatures and minimal wind with the heat source's thermostat set at point at 68°F. Thermography was used during the tests to supplement the temperature data points. The manufacturer's system had corresponding (normally aligned) interior and exterior thermocouple sites on the center of its lower glass pane and the center of its middle mullion. The five systems were similarly instrumented so that side-by-side comparisons could be made with the manufacturer's system. Lastly, interior air temperature was recorded at three mid-height locations in the enclosure along with exterior air temperature.

Calculating the apparent thermal resistance of the test units was accomplished with the equations below, derived from the principle of thermal resistance networks. In Eq.1, it is presented that given steady state conditions, absent thermal storage, heat flow conducting through the envelope assemblies equals the heat flowing into the assembly via convection and radiation (also noted in Figure 2). These heat flows can be represented in terms of resistances (in ft^2-h-°F/Btu units) and related temperature differentials (ΔT in °F).

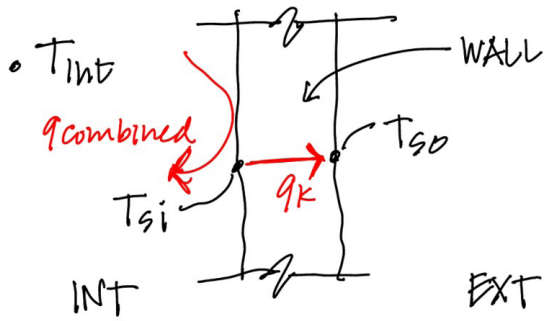

Figure 2: Diagram showing temperature sampling points used to calculate apparent envelope resistance.

Eq. 1

$$\frac{(T_{int} - T_{si})}{R_{conv+rad}} = \frac{(T_{si} - T_{so})}{R_{envp}}$$

Where: T_{int} = interior ambient temperature
T_{si} = envelope surface temperature, interior
T_{so} = envelope surface temperature, exterior
$R_{conv+rad}$ = convective and radiative resistance, combined
R_{envp} = envelope conductive resistance

The resistance network equation can be then rearranged to solve for envelope conductive resistance, as shown in Eq. 2.

Eq. 2

$$R_{envp} = \frac{(T_{si} - T_{so})\,(R_{conv+rad})}{(T_{int} - T_{si})}$$

The components of Eq. 2 demonstrate the environmental parameters required to calculate envelope conductive resistance: a stable interior temperature, the corresponding interior and exterior surface temperatures, and the combined convective and radiative resistance for the interior environment. Note that exterior air temperature is not required in this equation, though in testing, exterior temperature was logged to ensure that for a given segment of time exterior air temperatures remained stable to maintain relatively steady state heat loss. It may also be noted that (T_{int}-T_{si}), the difference between interior ambient temperature and interior envelope surface temperature, is a factor (mathematically) in the calculation of envelope resistance. In lieu of calculating this resistance, the relative magnitude of various observed temperature differentials correlates closely to the calculated resistance, although only calculated resistance is presented in the results (Table 2).

Surface temperatures T_{si} and T_{so} were taken directly from thermocouple data sampled every 10 seconds. The interior temperature, T_{int}, was established as the average value from three locations within the enclosure. Temperatures from these three points remained very close throughout the tests, to around 0.5 °F, although due to the nature of the heating source, temperatures would

[iv] Thermocouples were adhered to surfaces using aluminum tape spray-painted either black or white to reduce the effects of radiant heat loss on local temperatures, and thermal imagery confirmed temperature uniformity around thermocouple locations during testing. Data acquisition devices recorded synchronized data from all channels on a laptop computer at five second intervals. Individual thermocouples were calibrated using ice point calibration prior to testing, and a specific correction applied to every thermocouple according to this calibration. The heater was directed away from the curtain wall prototypes in the interior and because of the small size of the heater, forced convection had a negligible effect on the individual prototypes and sensors.

rise and fall at intervals (typically 30 to 40 minutes, changing dependent on the exterior temperature). This is a departure from typical test enclosures that would have constant temperature control rather than on/off cycling. As a result of these temperature cycles, and the variation in response at the various thermocouple sites, calculations presented used the most local interior air temperature to a given surface temperature sampling site, and instantaneous resistances were calculated and then averaged for a two minute period. The criteria for setting this period involved identifying a two-minute period (containing 12 temperature samples) within the off cycle of the heating system, a time period most closely representing steady state heat loss through the envelope (Figure 5). Three two minute intervals were analyzed in this way, and the resulting resistances were averaged to determine an average R_{envp} value for each sampling site (Table 2).

Having thus far established the methods and intent of collecting temperature samples, the question of heat transfer at the interior envelope surface must be addressed. Recalling Eq. 1 and Eq. 2, $R_{conv+rad}$ is the resistance of the air at the surface of the interior envelope where heat is being transferred from the air to the envelope wall. For the purposes of the experiments, this resistance factor accounts for convection and some amount of radiation, although radiative transfer in the test enclosure is minimized due to the reflective interior surfaces of the enclosure walls[v]. The resistance factor $R_{conv+rad}$ is the inverse of the combined coefficient of convection and radiation (h_{conv}, with units Btu/ft^2-h-F) and plays a critical role in determining the apparent resistance of an enclosure is quite critical, while these values under ambient indoor conditions can vary widely. Indoor values for h_{conv} may fall roughly between 1 and 5 Btu/ft^2-h-F as a textbook reference, however, in precise scientific experiments requiring this value the experimenter is typically obliged to determine the value of h_{conv} by in situ observation, under the exact conditions of the planned experiment. While some part of h_{conv} can be attributed to the surface characteristics of the materials upon which the air is convecting, it should be emphasized that this is a property of the air and the surrounding environment. Thus in the case of the test enclosure, a generalized h_{conv} value may reasonably apply to all of the heat transfer cases in the envelope because each temperature sampling sites involve similar, adjacent surfaces.

If the experimental methods included heat flux sensors, the need to calculate h_{conv} would be moot because the sensors would yield instantaneous heat flux (heat transfer rates) and, along with the same temperature values discussed above, the resistance of the wall could be calculated without further effort. In the absence of heat flux sensors, h_{conv} must be determined another way. Coincidentally, the need to "fill in" this information is a major stumbling block in the effort to directly glean information on thermal resistance from only temperature data. For example, a previous study used systematically attained thermography to calculate the in-situ apparent R-value of complex wall systems, after they had been executed[6]. The study remarked at the disparity between very low apparent R-values calculated by field measurements versus the R-value determined by computer analysis; yet this methodology (referenced from sources in the thermography field) used an h_{conv} of 1.471 Btu/ft^2-h-F ($R_{conv+rad}$ of 0.68 Btu/ft^2-h-F), a value taken from standard air film resistances cited by ASHRAE[6]. While the goals of the Payette study are insightful – to better understand the relationship between heat transfer and architectural detailing – using a generic air film resistance intended for another purpose (determining assembly R-values by summation) is problematic when calculating for observed conditions where the air film and convection coefficient may be very different. Moreover, standards set in simulation software such as THERM (also used in[6]) apply much lower rates for the convection coefficient (for metal window frames, an h_{conv} of 0.549 Btu/ft^2-h-F and for glass surfaces an h_{conv} of 0.375 Btu/ft^2-h-F). Lower convection coefficients suggest a reduction in heat transfer by convection, so it is no wonder THERM results and calculations using the generic number do not agree.

After temperature data was initially collected, the combined coefficient for convection and radiation was determined experimentally by conducting a series of tests in the test environment. An aluminum bar of known physical and dimensional properties was heated and cooled, with intervals in between to allow the bar to reach equilibrium with the environment of the test enclosure. Conditions during the tests approximated the interior conditions during earlier thermal testing (an interior temperature in the mid-60s F), but the heating system was not operated during the these tests. A thermocouple was mounted to the aluminum bar and a second thermocouple was suspended a few inches

[v] Radiation would be an increased factor if surface temperatures in the environment would be greatly different. However, temperatures were within a rather tight range. Also, the surfaces that would exchange the most heat by radiation would be normal to the prototypes on the interior and the foil-faced surfaces of the SIPs would also greatly reduce radiative heat transfer.

from its surface. Each test began outside the enclosure, where the bar was either heated by a heat gun or chilled in an ice bath and then quickly brought into the test enclosure and positioned. Temperature readings of the bar were logged every second until the bar reached the temperature of the surrounding environment. Analyzing the drop in temperature across a given timestep throughout warming or cooling of the bar was then used to calculate the time constant of convective heat transfer. The following equation (Eq. 3) was used to determine the time constant from temperature data, a process referenced in[7]:

Eq. 3

$$\Delta T(t) = \Delta T_o e^{-t/\tau}$$

Where: $\Delta T(t)$ = difference in temperature at time increment t

ΔTo = initial temperature difference at t=0
t = time increment
τ = time constant
e = Euler's number

Using Microsoft Excel, temperature drops across time steps of 30 secs were plotted, and an exponential function (y=Ae-B/x) was graphed to the plot[vi]. The inverse of the constant in the resultant function established an approximation for the time constant τ. Two cooling off and two warming up tests were conducted, and the time constant calculated for each of the four tests. Having determined the time constant, it was then possible to calculate h_{conv} using Eq. 4 and the known material and geometric properties of the aluminum bar. It should be noted that the data analyzed to determine the time constant was using 30-second steps; this requires a conversion factor of 120 in introducing the time constant to Eq. 4 where the final units of h_{conv} use hours. The tests to establish the time constant and coefficient of convection and radiation thus yielded the values shown in Table 1, with close agreement among the four tests in arriving at a suitable value for h_{conv}. The values for h_{conv} could then be used in Eq. 2 to calculate the apparent thermal resistance of the assemblies, understanding that the inverse of h_{conv} is equivalent to $R_{conv+rad}$. It may be noted that the average value of 2.81 Btu/ft^2-h-F for h_{conv} is within the expected range of 1 to 5 Btu/ft^2-h-F, although it is a higher rate of convection (i.e. less resistance) than those discussed from THERM parameters and from typical values attributed to interior air films when considering R-Value summations.

Eq. 4

$$h_{conv} = \frac{m\,c}{\tau\,A}$$

Where: m = mass of the aluminum plate
c = specific heat of the aluminum alloy
τ = time constant, converted to hours
A = surface area of the aluminum plate exposed to convection

Table 1: Thermal constant values (τ) and the resultant values for h_{conv} calculated from experiments in the test enclosure. These values were used, along with temperature data, to calculate apparent R-values for the assemblies tested.

	τ (30 sec)	h_{conv} Btu/ft2.h.F
Cooling Test A	9.3	2.67
Cooling Test B	8.5	2.95
Heating Test A	8.7	2.87
Heating Test B	9.1	2.75
	h_{conv} average	2.81

[vi] The graphs in Figure 3 show plots that were used to calculate a value for combined convective and radiative heat transfer (h_{conv}) at the interior wall of the prototypes. A bar of aluminum was either heated or cooled above ambient temperature, and its heating or cooling to equilibrium was recorded in five second intervals while it was inside the enclosure. A temperature difference (the Y axis) for time steps of 30 seconds was then calculated from these heating or cooling curves in order to determine the thermal constant for heat loss and gain in the test enclosure environment. The exponential equation fit to each plot was used to determine the time constant, according to Eq. 3. Heating up of the aluminum from a cooler temperature is the most difficult process to measure because of the fast response of the aluminum – however this was done to demonstrate that the thermal constant applies to both heating and cooling.

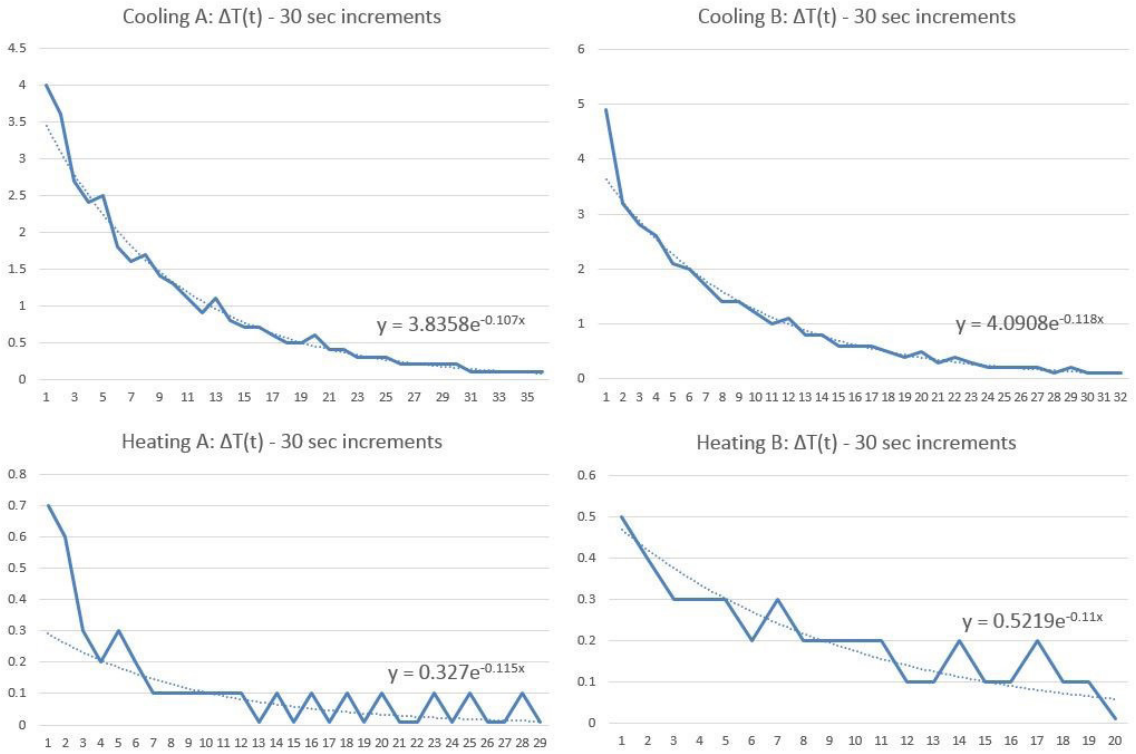

Figure 3: Temperature difference (the Y axis) for time steps of 30 seconds, plotted from tests showing the heating and cooling of an aluminum bar within the test enclosure environment.

3.4 Testing Infiltration

In addition to monitoring temperature data to calculate envelope resistance, tests were also conducted to measure infiltration (air leakage rate) for each prototype at -50 Pa and -75 Pa depressurization. Testing used a micro-controlled blower door kit, with the blower unit mated directly to the test enclosure. Masking of the prototypes involved applying masking tape to the perimeter shim area of each curtain wall prototype to exclude these gaps from the infiltration tests, given that the subject of the tests were the tightness of the glazing-to-frame interfaces within the prototypes. Thus infiltration results would represent the systems' deployment as a continuous, stick-built curtain wall system rather than a unit inserted into a wall. Masking and testing protocols referenced ASTM E783-02, using heavy poly sheet to seal off surfaces that were not part of the subject area for a given test[8]. The poly sheet also provided visible verification of negative pressurization within the test enclosure. The first infiltration test masked off all of the prototype systems using poly sheet; this initial test determined a baseline infiltration rate for the enclosure minus the prototype systems. Individual infiltration tests could then be carried out for the prototypes simply by unmasking them one at a time. Further discussion regarding the setup of the infiltration tests is discussed below[vii].

[vii] Infiltration tests referenced ASTM E783-02 (2010)[8]. Following this standard, "extraneous" gaps around each prototype were masked using masking tape to ensure only internal air leakage (around IGUs and in between frame connections) were measured. When a prototype was being tested, the other five prototypes were covered with five mil polyethylene sheet, taped to the exterior of the glass units. Data was recorded after the polyethylene sheet was "sucked" to the surface of the other prototypes, indicating complete negative pressure was achieved inside the test enclosure. Testing used a duct testing apparatus joined directly to the test enclosure, and tests were conducted at -50 Pa and -75 Pa and used an average of three 120-second averaged recorded by the testing instrument.

4.0 EXPERIMENTAL SYSTEMS AND FINDINGS

Fabricating and testing the prototypes at full scale was important in understanding their viability against real-world conditions and concerns. Three experimental systems along with the base system from the manufacturer are compared in this article, with their conceptual bases and findings from simulation and testing discussed.

4.1 Base System: 250xpt System from Collaborating Manufacture

The system provided uses aluminum frame with an internal polyamide thermal break to fully isolate the exterior pressure plate and cap from the interior frame (Figure 4). The glazing unit used was a triple glazed, argon-filled IGU with Low-E glass and structural silicone spacers and a factory edge seal, installed with EPDM gaskets on interior and exterior in the curtain wall frame (Figure 1). Joints in the assembly of the frame were friction-fit with factory-supplied hardware and further sealed with silicone. This system is the manufacturer's best performing curtain wall product, with performance on par with other top-of-the-line glass curtain walls. It should be noted that the base system was assembled in the factory by an experienced fenestration contractor as part of a demonstration organized for the students, while the experimental systems were devised in part or wholly in the college shop.

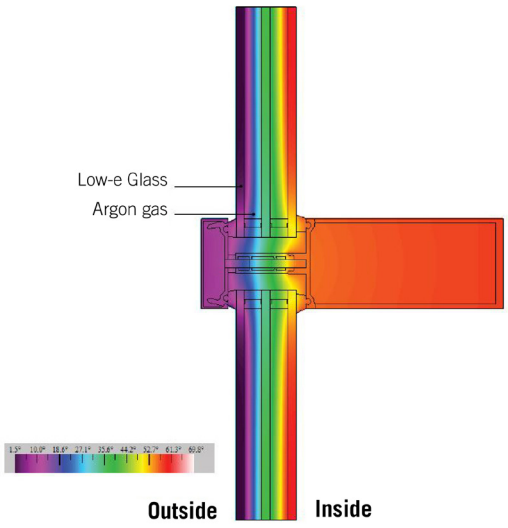

Figure 4: The collaborating manufacturer's 250xpt system with triple glazing and thermal break.

The manufacturer's system is also discussed in some detail along with the other systems, but testing yielded impressive results in both apparent thermal resistance and air leakage. With respect to apparent thermal resistance (Table 3), the glass was within 50 percent of the calculate R-Value from THERM (Table 2) with the value of h_{conv} likely part of the discrepancy. The sampling point of the frame yielded a higher than expected local resistance in the center of the frame, although R-Values from THERM account for the total values along the profile. In terms of apparent resistance, the 250xpt's triple glass unit also performed very closely to the students' System B (Composite Node) that used a deep, insulated airspace with two multiwall polycarbonate skins (each rated at R-2.5). In infiltration tests, leakage in the manufacturer's unit was nearly immeasurable at -50 Pa, bettering all the students' prototypes that used stick-built assembly techniques (Table 4). It may also be remarked that if the 250xpt's tested -75 Pa infiltration rate (0.06 cfm/ft2) could be maintained across an entire building envelope, it would well exceed the "best achievable" tightness (0.04 cfm/ft^2 @75 Pa)[3]. In sum, the manufacturer's system set a high performance bar for the student systems.

4.2 System A: Structural Spacer in Insulated Glass Units - Developed by: Tyler Countess, Hanh Phung, Samantha Wai

This system was developed by a team that acknowledged a conventional curtain wall frame is not used to its full structural capacity in the horizontal direction, merely transferring loads from the glass to the higher-loaded vertical mullions. The team also recognized that curtain wall frames have lower thermal resistances than modern IGUs, so eliminating any framing in the overall system would increase its thermal resistance. In response the team integrated a horizontal steel member within the top and bottom of the IGU that served both structurally and as a spacer (Figure 4). The spacer designed by the team is capable of spanning six inches in a 24 ft^2. IGU according to structural calculations for resisting dead load and wind loads and given the allowable deflections in the glass and adhesives. Two internal films within the slightly wider glass unit restrict convection. Computer simulations were carried out with the IGU using an argon fill and Low-E films, while the prototype constructed by the team was filled with air and used uncoated Mylar films. Vertical framing in the system used a shelf bracket to transfer loads from the now-structural IGUs to frame, while using conventional pressure plates and covers to complete the installation. A compressible foam gasket and silicon seals the hori-

zontal joints between IGUs resulting in a visible joint of only about 1/4 inch.

Virtual testing in THERM indicated an increase in thermal resistance of 59 percent compared to the base system, a significant improvement (Table 2). It appears that much of this improvement comes from an elimination of surface area at the frame where mullions have been eliminated. Though the thermal resistance at the structural space actually decreases, this is locally a much smaller area for heat transfer than the conventional mullion. Improved thermal properties were then simulated with whole building energy modeling (Autodesk Ecotect) in a 24,000 ft^2 commercial building. In comparative simulations, combined HVAC energy usage was reduced by 17 percent using this system versus a high-performing double glazed system. Secondly, the research team also used Ecotect to simulate the improvements to daylight factor offered by their system versus the base system; in a room with a 2:1 depth to height ratio, daylight factor increased 20 percent.

In prototype testing, the system performed quite well despite some compromises in the prototype materials: namely in the improvised IGU, which used uncoated Mylar rather than a low-E coated film, and also used air in glass unit rather than argon. Despite these compromises the glazing unit performed very closely to the manufacturer's base unit, with apparent thermal resistance slightly increased over the 250xpt mockup. Although apparent resistance at the center joint was much less than the 250xpt's center mullion, thermography confirmed that areas of increased transfer at structural mullion were much more isolated: a similar comparison as that drawn from THERM modeling. As an estimation, the observed resistances (Table 3) can be multiplied by the profile length of these two joints: the 250xpt's would conduct at 0.40 Btu/h per foot of mullion (R-2.18 * 10.5" of profile), while the structural mullion would conduct at merely 0.28 Btu/h per foot of joint (R0.45 * 1.5" of profile). While not measured, light admittance and view through the small prototype was increased notably in comparison to the more bulky conventional center mullion in the manufacturer's unit.

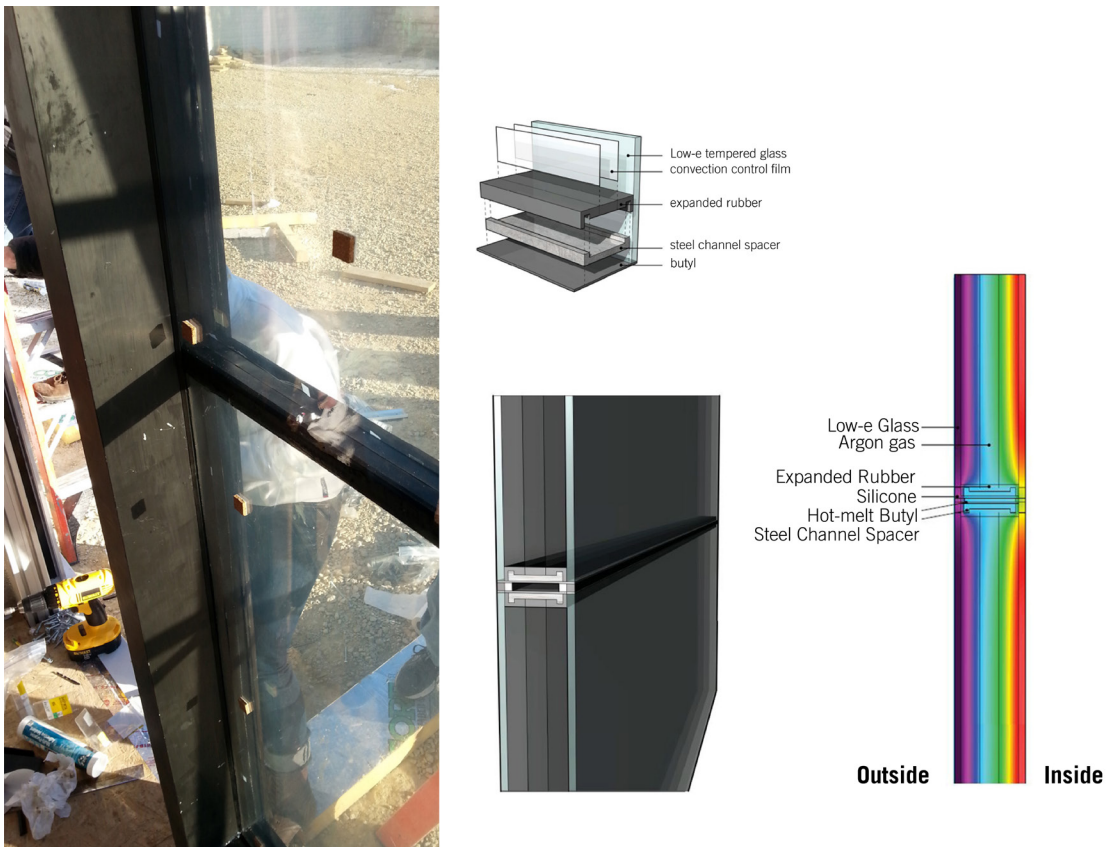

Figure 5: System A prototypes and thermal simulation.

During infiltration testing, the prototype suffered from assembly shortcomings in the glazing unit seals and Mylar interlayers, yet the system was tighter than the test enclosure (Table 4) and did not appear to leak through the horizontal joint. Industrial assembly methods would certainly improve the infiltration resistance of this system.

4.3 System B: Composite Node System - Developed by: Brian Conklin, Nick Nelson, Dylan Rupar

A team of students developed the composite node system in response to two strategies. First, the team adopted low cost, thermally insulating multiwall polycarbonate as an exterior and interior skin, separated by a framing system that would allow for a deep cavity of translucent polymer fiber insulation to increase overall thermal resistance. The second development in the system involved the frame itself. Rather than using a 10 inch deep aluminum profile, the team devised a system consisting of interior and exterior "rails" that could receive either polycarbonate or conventional IGUs and could be finished with conventional pressure plates and caps. Nodes of low conductivity laminated wood intermittently tie the rails together and connect the system back to building structure. Weather stripping, mechanically installed pressure plates, and conventional sealants complete the air and water barrier on the exterior face, with the interior wall left unsealed to allow periodic equalization of vapor from within the wall cavity.

One of the most important implications of this system is that aluminum is used in an advantageous manner: it remains an easy-to-erect system of components yet thermal conduction is reduced and the amount of aluminum overall is reduced. Further, the system could use more affordable non-appearance grade coatings for the rails, allowing with it the use of recycled aluminum instead of virgin aluminum.

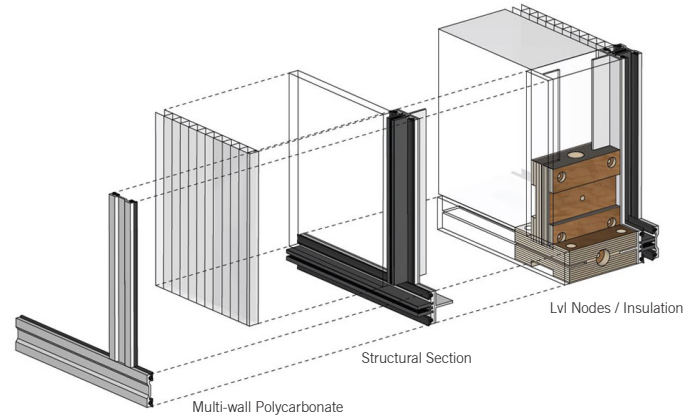

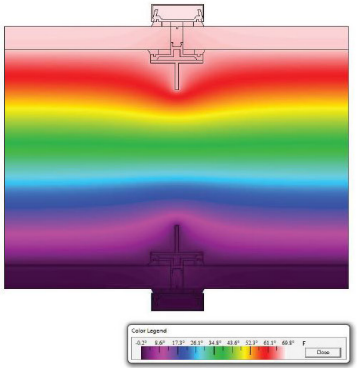

Heat Transfer at Cavity

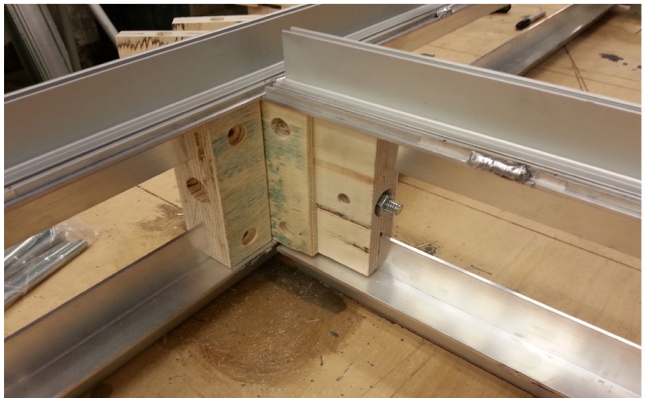

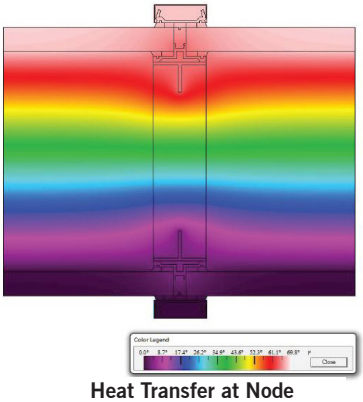

Heat Transfer at Node

Figure 6: System B diagrams and thermal simulations.

Simulations in THERM show that thermal resistance of the infill system with a six inch deep cavity would increase by a minimum of 65 percent at node connections to a maximum of 84 percent in the cavity areas of the system (Table 2). Whole building energy simulations were then used to compare performance of the 24000 ft^2 test building using this system versus the manufacturer's base system. With an aggregated U-Value for a composite wall of 20 percent glazing and 80 percent polycarbonate infill, building HVAC energy usage is reduced by 20 percent. The team also conducted several daylight simulations using Radiance to evaluate the impact of their system for daylight diffusion, distribution, and glare prevention.

Refinement of the team's node and raid system was aided by prototyping during the design process and aluminum rails in the final 1:1 prototype were improvised by welding standard curtain wall parts to aluminum "T" sections to create the system's cross profile. The nodes were milled and machined from laminated composite wood using CNC equipment and the final design used universal nodes (i.e. all node connections were made with the same components). The team's IGU, caps, pressure plates, and weatherstripping were provided by the manufacturer. Multiwall polycarbonate was sourced by the team from a local hardware store and the system substituted loose polyester fiber for translucent insulation batting for the cavities, the latter reducing the thermal resistance of the system. The system performed well in live testing, with higher apparent thermal resistance in the frames and polycarbonate than the manufacturer's system, although the margins were slimmer than expected from THERM tests (Table 3). In summary, the testing of the prototype confirmed expectations from computer simulations and showed that the main strategies of the system to reduce thermal transmission were working as expected. Infiltration tests were telling as well, with infiltration rates much lower than the SIP envelope of the test enclosure and lower than other groups' prototypes (Table 4). While not as tight as the manufacturer's system, this prototype had many more parts and opportunities for leakage and yet still performed well, demonstrating that the system's depth and double wall construction could pay off with airtightness and excellent thermal resistance.

4.4 System C: Structural Foam Composite - Developed by: Kate Gutierrez, Kristina Johnson, Jenelle Tennigkeit

The final system discussed in this article was developed by a group interested in unitized curtain walls and non-linear construction, versus stick systems that are assembled in the field from separate frame and glazing components. The group reasoned that framing systems were a liability for glass curtain wall systems, and often these facades were not entirely clear glass anyway with many installations using opaque, spandrel glass units. The solution devised by the group was to eliminate the aluminum framing altogether, replacing the glass support system with structural foam panels where glass units would be directly glazed using silicon adhesive. With a thin exterior skin of fiber-reinforced composite, the team calculated that IGUs of 50 ft^2 or more could be supported within a foam panel spanning floor to floor. Such foam panels can reduce the weight of conventional glass and infill panel systems by 60 percent, reducing construction equipment requirements and emissions in transportation. Details developed with the system included a concept for using cam locks to realize a tight seal against the building and adjacent panels to reduce infiltration, and a lapped interface between glass and panel that would maximize sightlines while reducing sharp thermal gradients that could result in condensation. Devised to demonstrate the concept of an "active Z-axis", the 1:1 prototype was CNC milled with a faceted profile facing the exterior: a strategy that could be applied in real applications to increase the structural rigidity, control surface runoff, or provide light control.

In the computer simulations (Table 1) and in live testing, this system showed a high degree of thermal resistance, as expected from the depth and foam composition of the panel. Given the relatively low thermal gradient, and the high resistance of the panel, the calculated thermal resistance was also the most inconsistent across the three testing intervals. Coincidentally the glass IGU, a double-glazed Low-E unit, recorded colder temperatures than any other glass surfaces during testing, perhaps because its recessed position in the deep panel where a cold pocket of air could develop. Whole building energy simulations using the 24,000 ft^2 base building, with an aggregate U-Value for a composite wall of 25 percent glazing and 75 percent opaque infill, showed a potential reduction in HVAC energy usage is reduced by 12 percent. The performance of this team's system is highly design-dependent and in a building where the spatial and functional impact of the wall is favored over glazing, greater energy reductions could be realized. Predictably, the monolithic nature of this system performed well in infiltration tests, showing no measured leakage at -50 Pa (Table 4) and only minor leakage at -75 Pa.

Figure 7: System C prototype and thermal simulation.

Table 2: Thermal performance of the tested systems versus the manufacturer's triple-glazed system, as tested using THERM and WINDOW software with NFRC testing parameters applied.

Comparison of Thermal Performance:
THERM and WINDOW Simulations w/ NFRC Guidelines

System	Window Assembly U-Value, Glass and Frame, Btu/h-ft^2-	Infill System U-Value, Btu/h-ft2-F
Mfr's 250xpt	0.29	N/A
System A: Structural Spacer	0.128	N/A
System B: Composite Node	0.29	0.11 (node intersections) 0.05 (max, cavity ctr)
System C: Foam Composite	0.29	0.025

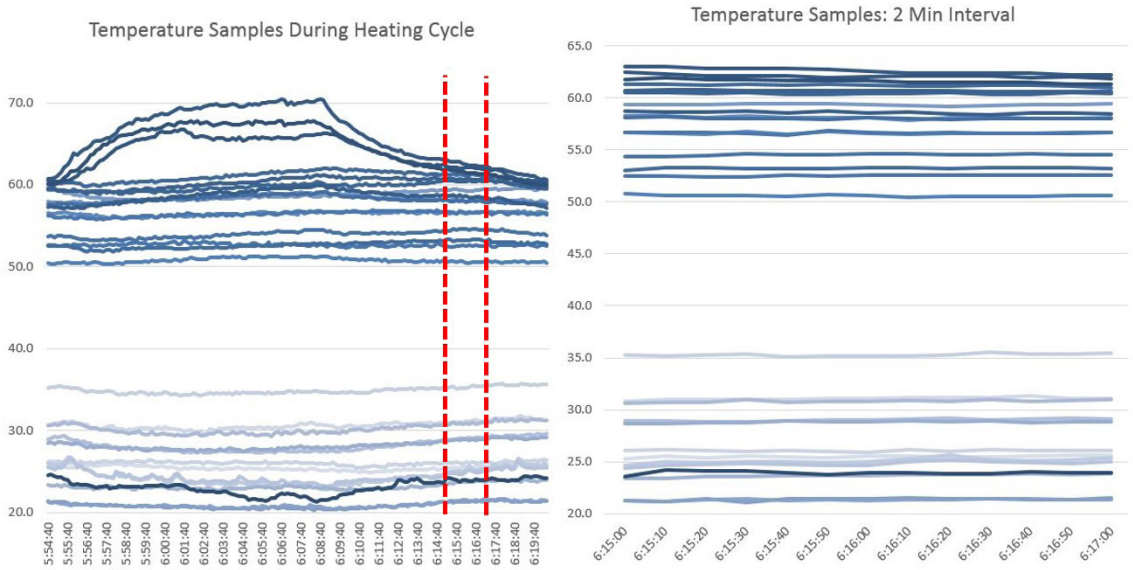

Figure 8: An example of temperature plots from prototyping testing, part of three separate tests conducted over periods of several hours to multiple days. At left shows temperatures through a single heating interval of approximately 25 minutes, with the top three plots representing interior air temperature, and the lowest plots exterior surface temperatures. The section of data yielding the two-minute interval is demarked between vertical lines. At right is the two-minute interval used for calculating apparent thermal resistance of the various systems, showing conditions close to steady-state during the interval.

Table 3: Apparent envelope resistance of the tested assemblies. Testing intervals (A, B, and C) of 120 seconds were taken from three respective tests. Apparent resistance was calculated using Eq. 2.

Apparent Envelope Resistance, R_{envp} h.ft².F/Btu

	Ave, Interval A	Ave, Interval B	Ave, Interval C	Ave, Total
Center of Middle Mullion				
Mfr's 250xpt (Mullion)	2.20	2.19	2.15	2.18
System A - Structural Spacer (IGU at Spacer)	0.46	0.44	0.45	0.45
System B - Composite Node (Mullion)	2.67	2.53	2.56	2.58
System C - Foam Composite (Solid)	28.92	23.65	16.44	23.00
Center of Lower Panel				
Mfr's 250xpt (Glass)	3.59	3.76	3.75	3.70
System A - Structural Spacer (Glass)	1.74	1.74	1.82	1.77
System B - Composite Node (Polycarbonate)	3.77	4.05	3.56	3.79
System C - Foam Composite (Solid)	13.19	16.94	9.98	13.37

Table 4: Infiltration tests conducted for each system. The baseline infiltration rate of the test enclosure represents the rate of the entire envelope of enclosure with the tested systems masked. Negative pressures of 50 pascals and 75 pascals correspond to common depressurization values used in building commissioning.

Infiltration Tests

Configuration tested	@-50 Pa	@-75Pa	CFM/ft² @ -50Pa	CFM/ft² @ -75Pa
All systems masked - baseline	199.9	259.0	0.39	0.51
Mfr's 250xpt	0.1	0.9	0.04	0.06
System A: Structural Spacer	4.6	6.9	0.30	0.45
System B: Composite Node	2.6	4.3	0.17	0.28
System C: Foam Composite	0.0	2.1	0.00	0.13

*The area of each system tested for infiltration was 15.47 square feet. The total surface area of the test enclosure, minus the area of the systems, was approximately 512 square feet.

5.0 CONCLUSION

Research applications involving the test enclosure is continuing at Kansas State in the Department of Architecture, with a new project involving a new system. With this new project, some improvements to data collection and analysis will be attempted[viii], specifically to improve prototype comparisons that are dependent on stable environmental conditions in the enclosure. Clearly for thermal resistance, the apparent thermal resistance measured in these in-situ tests will never perfectly match the ratings derived from controlled laboratory testing, it is anticipated that improvements to the experimental set up and methods will yield observations with more confidence and closer to expected values. Yet, despite discrepancies between apparent thermal resistances and simulated resistances, the experiments using the test enclosure yielded insightful results that were useful in making comparisons from system to system.

A larger goal of the work is thus to develop and perfect methods that are rigorous, in the sense of ASTM standard methods, yet can be achieved by designers and professionals – architecture students and architects interested in design and not just engineering conclusions – without highly technical laboratories. While there are challenges in achieving the testing rigor of ASTM standard methods, those cited in this article are methods proven for in-situ conditions, rather than labs, and we can use them as a starting point for practice-friendly methods, as long as these methods are based on sound building science fundamentals. For example, calculating an apparent convection coefficient (hconv) is perhaps a painful process, but a more informed approach than using a generic textbook value. As architects increasingly gain access to evaluation tools, such as simulation software and instruments like thermal cameras, adequate building science knowledge and rigor in methodology are critical in realizing the benefits of these tools to design.

Overall, the process of prototyping and experimentation resulted in a comprehensive knowledge of the thermal performance of curtain wall assembly systems, and how they could be improved. The first realization from the studio's testing was that the manufacturer's 250xpt

[viii] Several improvements will improve future experiments. The biggest improvement is expected to come from adding an always-on heating system that can control the interior temperature without cycling. This will stabilize interior temperatures near a steady state, and make localized air temperatures near sampling points more consistent. Secondly, adding more thermocouple channels will allow air temperatures to be taken closer to the sampling points, perhaps one air temperature reading for every interior surface temperature reading. The reality is that in an environment, air temperatures can be very dynamic and variations of a few degrees have a large impact on heat flow. Introducing one or several heat flux sensors into the experiments is also planned, though the hope is that accuracy can be improved with a thermocouple based method that is more affordable and easier to manage.

system is indeed quite remarkable at resisting thermal flows, setting a challenging bar for the students' systems to exceed. For example, System B (Composite Node), with a deep insulated airspace and two layers of multiwall polycarbonate, might be picked to easily surpass the 250xpt with its glass and conventional framing system; however, the performance of the two systems were very close. The airtightness of the 250xpt was also impressive, showing how a controlled, industrialized system can meet its performance objectives when it is assembled and installed correctly. Given the performance capability of modern curtain wall systems, these systems can be logically integrated, rather than avoided as a liability, for innovative low-energy buildings. Some important performance advantages were demonstrated by the student systems, as discussed already. With some improvements to prototypes, performance could increase further towards the outcomes predicted by computer analysis, this would include using the same simulated materials and profiles (and specifically, materials with available reference properties) in the prototypes and improving student fabrication skills to level out the impact of construction and installation quality. Additionally, the three student systems would show an even greater degree of advantage if they were compared to code-minimum curtain wall systems, instead of the "green flagship" system represented by the 250xpt. While economics was not a part of the studios' analysis of experimental systems, any of these three systems could arguably be manufactured affordably and reasonably, possibly even as an initial trial emerging from direct collaboration between manufacturer, architect, and consultants.

While the process of prototyping and testing (including the computer tools and analytical methods) in this project came from an academically-based research effort, this process could also take place as part of real world practice. As discussed earlier, architecture firms are acquiring tools for evaluation and have the ability to use methodical analysis to better inform design decisions. Builders already build 1:1 prototypes for architects for some level of aesthetic, quality, or water testing: certainly these prototypes could be used for thermal and infiltration testing. With commissioning and other performance-related imperatives becoming more common, it is evident that testing prototypes is advantageous, rather than the final product where failure is costly.

Lastly, the role of curtain wall manufacturers in assembling products from an amalgam of proprietary materials from other manufacturers is worth highlighting from the studio's work. It may seem remote that a manufacturer adopt a system whose disparate material components must come from several different outside sources, like the Composite Node System discussed in this article. Yet this is exactly what curtain wall manufacturers do: they do not handle raw materials to make anything, but purchase component materials from other sources to produce a finished product including glass, aluminum profiles, gaskets, thermal breaks, coatings, spandrel infill materials, integrated shading devices, and many other individual components are sourced from others to create a "product" for any given manufacturer. Thus it might be argued that the next horizon in high-performing curtain wall systems are simply new, better performing composites of existing components.

Acknowledgements

The author would like to thank Manko Window Systems and Kevin Dix, PE and Vice President of Manko, for generously working through the process of inquiry, design, and prototyping with the student teams involved in this research and for providing the glazing components and glass for the prototypes.

Brian McKinney and Nadav Bittan, of BNIM architects in Kansas City, and Rick Shladweiler of PGAV architects in Kansas City also contributed their time and collaborative efforts for crits and reviews during the research process.

This research work was also sponsored by an NCARB Award for the Integration of Practice and Education. Funding from the award was used almost entirely for materials to build the test enclosure, for student prototypes, and for new equipment that supported this research.

Lastly, the author is indebted to the extensive efforts of the students involved, acknowledging the enthusiasm, curiosity, knowledge base, and persistence that is needed to bring serious research into the design studio. The participating students were: Brian Conklin, Tyler Countess, Kate Gutierrez, Kristy Johnson, Cameron Marshall, Jose Martinez-Giron, Nick Nelson, Nathan Niewald, Alex Otto, Kevin Perks, Hanh Phung, Dylan Rupar, Lawrence Tan, Jenelle Tennigkeit, and Sammi Wai. The author would also like to thank the Department of Architecture and the College of Architecture, Planning, and Design for the opportunity to teach this funded studio.

REFERENCES

[1] Gibson, M. D., (2015). "Designed for Performance: A Collaborative Research Studio Rethinks Glass Curtain Wall Systems", *Future of Architectural Research -- Proceedings of the ARCC 2015 Research Conference*, Aksamija, A., Haymaker, J. and Aminmansour, A., eds.: Chicago, IL, April 6 – 9.

[2] Boyle, B. J., Runkle, J., and Ziegler, R., (2013). "Achieving Tight Buildings through Building Envelope Commissioning", *Proceedings of the 3rd AIVC Airtightness Workshop*, Washington DC, April 18-19.

[3] Emmerich, S., McDowell, T., and Anis, W., (2005). "Investigation of the Impact of Commercial Building Envelope Airtightness on HVAC Energy Use", National Institute of Science and Technology.

[4] ASTM C1046-95, (2013). Standard Practice for In-Situ Measurement of Heat Flux and Temperature on Building Envelope Components, West Conshohocken, PA: ASTM International.

[5] ASTM C1155-95, (2013). Standard Practice for Determining Thermal Resistance of Building Envelope Components from the In-Situ Data, West Conshohocken, PA: ASTM International.

[6] Love, A., and Klee, C., (2014). "Thermal Bridging: Observed Impacts and Proposed Improvement for Common Conditions", *Proceedings of BEST4 Conference Building Enclosure Science & Technology*, Kansas City, MO, Retrieved from http://www.brikbase.org/content/thermal-bridging-observed-impacts-and-proposed-improvement-common-conditions on 7/25/2015.

[7] Conti, R., Gallitto, A., and Fiordilino, E., (2014). "Measurement of the Convective Heat-Transfer Coefficient", arXiv; Cornell University Library Database, Retrieved from http://arxiv.org/pdf/1401.0270.pdf on 6/10/2015.

[8] ASTM E783-02, (2010). Standard Test Method for Field Measurement of Air Leakage Through Installed Exterior Windows and Doors, West Conshohocken, PA: ASTM International.